Journal of Thermal Analysis and Calorimetry, Vol. 67 (2002) 699–712

THERMAL INVESTIGATIONS OF $M[La(C_2O_4)_3]\cdot xH_2O$ (*M*=Cr(III) AND Co(III))

N. Deb

Department of Chemistry, North Eastern Regional Institute of Science and Technology, Nirjuli 791109, Arunachal Pradesh, India

(Received December 1, 2000; in revised form May 8, 2001)

Abstract

The complexes $M[La(C_2O_4)_3]\cdot xH_2O$ (x=10 for *M*=Cr(III) and x=7 for *M*=Co(III)) have been synthesized and their thermal stability was investigated. The complexes were characterized by elemental analysis, IR, reflectance and powder X-ray diffraction (XRD) studies. Thermal investigations using TG, DTG and DTA techniques in air of chromium(III)tris(oxalato)lanthanum(III)decahydrate, $Cr[La(C_2O_4)_3]\cdot 10H_2O$ showed the complex decomposition pattern in air. The compound released all the ten molecules of water within ~170°C, followed by decomposition to a mixture of oxides and carbides of chromium and lanthanum, i.e. CrO_2, Cr_2O_3, Cr_3O_4, Cr_3C_2, La_2O_3, La_2C_3, LaCO, $LaCrO_x$ ($2<x<3$) and C at ~1000°C through the intermediate formation of several compounds of chromium and lanthanum at ~374, ~430 and ~550°C. The cobalt(III)tris(oxalato)lanthanum(III)heptahydrate, $Co[La(C_2O_4)_3]\cdot 7H_2O$ becomes anhydrous around 225°C, followed by decomposition to Co_3O_4, $La_2(CO_3)_3$ and C at ~340°C and several other mixture species of cobalt and lanthanum at ~485°C. The end products were identified to be $LaCoO_3$, Co_3O_4, La_2O_3, La_2C_3, Co_3C, LaCO and C at ~1000°C. DSC studies in nitrogen of both the compounds showed several distinct steps of decomposition along with ΔH and ΔS values. IR and powder XRD studies have identified some of the intermediate species. The tentative mechanisms for the decomposition in air are proposed.

Keywords: IR, oxalato, thermal decomposition, X-ray powder diffraction

Introduction

The complexes containing oxalate as ligand of both simple and complex types with transition and non-transition metals are classified and reviewed [1]. Many workers have studied oxalates of transition and non-transition metals of different types [2–7]. We also reported [8–18] exhaustive studies on a series of oxalato complexes of the type $M[M(C_2O_4)_n]\cdot xH_2O$ (*M*=same metal). Some workers also studied [19–25] the mixed metal oxalates keeping in mind the formation of mixed metal oxides and their possible applicability. Recently, we have reported [26, 27] the oxalato compounds of lanthanum of the types $M^1_3[La(C_2O_4)_3]\cdot xH_2O$ (M^1=Li, Na and K) where the end products of thermal decomposition were found to be mixture of oxides, carbides and

1418–2874/2002/ $ 5.00

Akadémiai Kiadó, Budapest
Kluwer Academic Publishers, Dordrecht

$MLaO_x$ (*M*=Li, Na and K). Nagase [28] investigated the phase transition of $K_3[Cr(C_2O_4)_3]$ from amorphous to crystalline state. Later on the same author [29] reported the decomposition of $K_3[Cr(C_2O_4)_3]\cdot 3H_2O$ in helium. X-ray structural analysis on $(NH_4)_2UO_2(C_2O_4)_2$ has been reported [30]. The compounds $Li_2UO_2(C_2O_4)_2\cdot 5H_2O$ and $Na_2UO_2(C_2O_4)_2\cdot 4H_2O$ are found [31] to decompose to monouranates through alkali metal carbonates and UO_2 as intermediates. The photosensitive rare earth trioxalatocobaltate(III) has been chosen [32] as a precursor for rare earth cobaltites(III), which manifest interesting electronic, magnetic and catalytic behaviour. The superiority of the catalytic activity depends [33, 34] on spin-state properties in the cobaltites. The citrate complexes as precursors have also been taken for the formation of $LaCoO_3$ and $LaCrO_3$ [35] through thermal decomposition. Although, the oxalato complexes of various types were studied, the photo insensitive compounds of lanthanum with transition metals were not reported. Therefore, in continuation of our recent work on mixed metal oxalato compounds [36] and keeping in mind the formation of mixed metal oxide as one of the end products and their possible catalytic applicability, the present study describes our attempts to investigate the mode of decomposition of chromium(III)tris(oxalato)lanthanum(III)decahydrate, $Cr[La(C_2O_4)_3]\cdot 10H_2O$ and cobalt(III)tris(oxalato)lanthanum(III)heptahydrate, $Co[La(C_2O_4)_3]\cdot 7H_2O$ in air and nitrogen. A tentative mechanism of the decomposition in air is proposed.

Experimental

The chemicals used were of AR grade purity. The preparative method is similar to the method adopted earlier [27, 36]. The compounds were filtered off, washed several times with distilled water and dried over calcium chloride. The chromium compound was isolated as light greenish and cobalt compound was light pink in colour. The water contents were determined gravimetrically and thermogravimetrically. Carbon and hydrogen contents were determined with a Carlo Erba 1108 elemental analyser.

IR spectra, diffuse reflectance spectra, thermal data (DTA, TG and DTG) at 10°C min^{-1} upto 1000°C, X-ray powder diffraction patterns were recorded as described earlier [17, 36]. DSC profiles were recorded on TA instrument DSC-2010 at 10°C min^{-1} in a dynamic nitrogen atmosphere.

Results and discussion

The complexes $Cr[La(C_2O_4)_3]\cdot 10H_2O$ and $Co[La(C_2O_4)_3]\cdot 7H_2O$ were insoluble in water or in common organic solvents, but decomposes in strong acid or alkali. The water analysis, microanalytical data and estimated metal contents were consistent with the proposed formula of the complexes. The selected bands (Table 1) in the IR spectra of the compounds suggested [17, 18, 36, 39] the chelating character of the oxalato groups.

Table 1 Selected IR bands (cm^{-1})

$Cr[La(C_2O_4)_3]\cdot 10H_2O$	$Co[La(C_2O_4)_3]\cdot 7H_2O$	Assignments
2800–3640 b (split into 2860, 2920, 3280)	2800–3680 b	ν_{sy}(O–H)+ν_{asy}(O–H) or hydrogen bonding
1620 S	1650 S	δ_{sy}(H–O–H)
1500–1760 b	1400–1820 b	ν_{asy}(C=O)
1465 m, 1380 m	1380 m	ν_{sy}(C–O) and/or ν(C–C)
1310 m	1330 m	ν_{sy}(C–O) and/or δ(O–C=O)
800 s	800 s	ν(M–O) and/or δ(O–C=O) or coordinated water
–	610 s	crystal water
–	540 vs	ν(M–O) and/or ν(C–C)
460 vs	460 m	δ(O–C=O) and/or ring deformation
360 vs	360 sw	δ(O–C=O)
280 vs	310 vs	π(out-of-plane bending)

s – small; vs – very small; w – weak; m – medium; S – strong; b – broad

The electronic spectrum of the solid sample of $Cr[La(C_2O_4)_3]\cdot 10H_2O$ displayed the bands around 16 800, 20 000 and 27 390 cm^{-1} due to spin-allowed transitions [37] and/or *d–d* transition, where the band at 20 000 cm^{-1} is assigned to $^4A_{2g}$ (F)→$^4T_{1g}$ (P) transition in distorted octahedral geometry of Cr(III). The bands observed at 38 900 and 46 500 cm^{-1} are due to ligand to metal charge transfer and π→π* transition respectively. The bands observed at similar position (16 800 and 20 000 cm^{-1}) in case of $Co[La(C_2O_4)_3]\cdot 7H_2O$ indicates a distortion from ideal geometry for octahedral Co(III) where the bands are due to $^1A_{1g}\rightarrow{}^1T_{1g}$ as well as *d–d* transition [10, 37]. Two additional bands at 33 300 and 46 500 cm^{-1} in the UV region are due to *M*→*L* or *L*→*M* charge transfer and π→π* transition respectively.

The XRD pattern (Tables 2 and 3) of the compounds differ from each other which indicates that they are not isomorphous.

TG, DTG and DTA curves of $Cr[La(C_2O_4)_3]\cdot 10H_2O$ are shown in Fig. 1. In TG curve, the mass loss starts from room temperature, and an inclined slope upto 170°C with 28.5% mass loss indicates the removal of all the ten molecules of water. The calculated mass loss to get the complete anhydrous species is 28.37%. A DTG change between 80 to 196°C, and an endothermic peak in the range 90–170°C (ΔT_{min}=125°C) in DTA correspond to the dehydration step. The precursor is heated upto 200°C in furnace and subjected to powder XRD and IR studies. Major differences in the *d*-spacing in the XRD data (Table 2) with the precursor is due to change in the internal structure on removal of both coordinated and crystal water. However, a few *d*-values are similar to *d*-spacing of the precursor, which indicates the retention of chelated oxalato groups. The IR bands also confirmed the retention of $C_2O_4^{2-}$ groups. The TG curve shows continuous mass loss, and 7.5% mass loss in a long temperature range

170–374°C (without change in DTA and DTG curves in the range) with overall mass loss of 36% indicates the partial decomposition of $C_2O_4^{2-}$ groups.

Table 2 X-ray powder diffraction (XRD) data of $Cr[La(C_2O_4)_3]\cdot 10H_2O$ and pyrolysed products at 200, 420 and 970°C in air

$Cr[La(C_2O_4)_3]\cdot 10H_2O$		Pyrolysed product					
		at 200°C		at 420°C		at 970°C	
d(Å)	*I*(Rel)	*d*(Å)	*I*(Rel)	*d*(Å)	*I*(Rel)	*d*(Å)	*I*(Rel)
7.082	78.79	5.001	100.00	6.609	73.64	5.738	83.62
4.936	100.00	4.224	94.08	3.446	100.00	3.300	78.21
3.583	42.57	2.941	80.74	2.523	65.35	3.225	100.00
2.831	42.87	2.103	56.96	2.184	55.97	2.295	53.13
2.343	38.81	1.702	46.40	2.050	48.10	2.051	40.23
1.549	20.18	1.573	46.39	2.019	59.45	1.880	61.04
1.392	20.09	1.548	52.02	1.615	41.37	1.649	24.52
1.219	13.64	1.330	32.87	1.560	38.23	1.610	29.30
1.134	13.88	1.220	25.43	1.532	42.18	1.462	24.74
1.086	13.48	1.134	30.96	1.363	37.01	1.352	28.01
1.036	11.77	1.098	24.98	1.277	35.40	1.235	26.80
1.009	13.70	1.064	22.89	1.184	31.05	1.148	18.65
0.979	12.63	1.008	32.10	1.088	24.52	1.067	22.10
0.951	14.20	0.988	27.60	1.067	29.30	1.079	16.50
0.885	12.41	0.923	27.14	1.044	26.58	1.042	20.12
0.839	14.95	0.903	25.83	0.998	24.11	1.035	14.71
0.814	12.99	0.885	20.93	0.959	28.96	0.971	14.72
0.801	14.12	0.854	26.68	0.906	25.58	0.937	16.33
0.788	16.33	0.838	30.76	0.858	29.90	0.878	16.78
–	–	0.822	28.24	0.843	34.40	0.848	17.68
–	–	0.810	32.19	0.808	42.10	0.844	19.28
–	–	0.790	33.43	0.796	33.57	0.833	19.84
–	–	–	–	–	–	0.820	21.38
–	–	–	–	–	–	0.811	17.93
–	–	–	–	–	–	0.791	22.67
–	–	–	–	–	–	0.787	20.68

The observed mass loss as against calculated value of 35.29% for $Cr[La(C_2O_4)_{2.5}]$ indicates its formation through reduction of Cr^{III} to Cr^{II} by $C_2O_4^{2-}$ group [17, 29] and evolved CO (*g*). Similar partial fragmentation was observed elsewhere [17, 38]. Further-

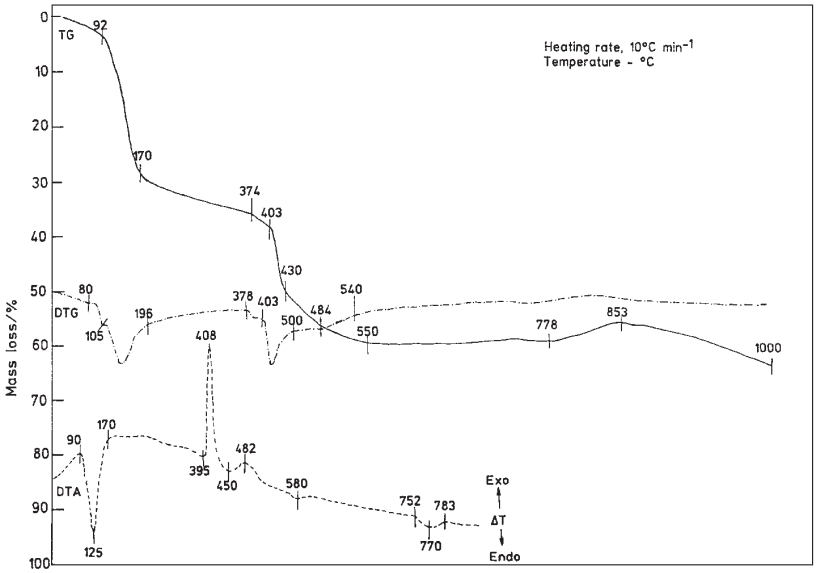

Fig. 1 TG, DTG and DTA curves of $Cr[La(C_2O_4)_3]\cdot 10H_2O$ in air

more, in TG a small distinct inclined step from 374 to 403°C (DTG change, 378–403°C) with 38% mass loss is ascribed due to the breaking of metal-ligand bond with evolution of CO (*g*) and CO_2 (*g*). The displayed steep slope from 403 to 430°C with a break (mass loss, 50%) which suddenly changes (through another break at 484°C with 56.5% mass loss) to an inclined nature upto 550°C with 59.5% mass loss gives credence to the formation of several transient intermediates. The mass loss at first break around 430°C supports the product may be either of mixture of $1/2La_2(CO_3)_3$ with CrO_2 (calcd, 50.57%) or with $1/2Cr_2O_3$ (calcd, 51.99%) or may be with CrO (calcd, 53.09%). An exothermic peak in DTA in the range 395–450°C (ΔT_{max}=408°C) corresponds to the above step. Although in TG curve the intermediates at 430°C immediately changes to some other products, we tried to obtain the pyrolysed product around the same temperature, and a black residue could be isolated at ~420°C after 51.20% mass loss.

The species gives the XRD peaks [42] (Table 2) for CrO and a few recorded for Cr_2O_3 and CrO_2 as well. It indicates, as soon as CrO is formed, a part of it oxidised immediately to Cr^{III} [17] and Cr^{IV} in air at the mentioned temperature. The presence of C is also detected [42] from XRD as it formed through disproportionation [26, 27] of CO (*g*) to CO_2 (*g*). The other *d*-spacing also confirmed the presence of La_2O_3, which is produced from the decomposition of a part of lanthanum carbonate moiety. The remaining mismatched *d*-values may be for undecomposed $La_2(CO_3)_3$. The IR bands of the residue at 1350–1555, 1030, 720, 645, 625 and 435 cm^{-1} further support [27, 39] their presence. The second break in TG at 484°C apparently indicates the formation of CrO, and oxycarbonate, $1/2La_2O(CO_3)_2$ (mass loss, found 56.5%; calcd, 56.71%) on decomposition of carbonate. A small exotherm at 482°C in DTA corresponds to the carbonate decomposition. The major decomposition step finished at 550°C in TG

Table 3 X-ray powder diffraction (XRD) data of $Co[La(C_2O_4)_3]\cdot 7H_2O$, and pyrolysed products at 257, 350, 510 and 970°C in air

$Co[La(C_2O_4)_3]\cdot 7H_2O$		Pyrolysed product							
		at 257°C		at 350°C		at 510°C		at 970°C	
d(Å)	I(Rel)	d(Å)	I/I_o(Rel)	d(Å)	I/I_o(Rel)	d(Å)	I/I_o(Rel)	d(Å)	I/I_o(Rel)
10.664	74.90	10.662	95	6.351	93	8.350	90	7.113	86
7.082	92.72	7.939	97	5.128	78	6.736	83	6.761	79
4.862	100.00	4.863	82	3.852	72	4.980	62	5.756	73
3.570	79.78	3.657	65	3.384	65	4.917	71	4.334	65
2.834	75.85	3.571	78	3.370	42	4.698	66	3.836	65
1.948	72.81	3.422	62	3.322	65	4.668	68	3.378	53
1.550	69.13	1.947	70	3.200	51	3.918	70	3.268	62
1.412	67.30	1.896	55	3.096	62	3.836	68	2.724	100
1.331	67.36	1.744	53	2.856	58	3.060	62	2.696	88
1.257	67.28	1.550	61	2.434	59	3.034	58	2.440	58
1.159	65.60	1.135	41	1.869	49	3.009	64	2.220	54
1.112	65.21	1.112	54	1.840	38	2.886	66	2.147	44
1.036	64.04	–	–	1.681	47	2.551	50	2.086	45
1.016	64.49	–	–	1.646	50	2.460	47	2.030	42

Table 3 Continued

$Co[La(C_2O_4)_3]\cdot 7H_2O$		Pyrolysed product							
		at 257°C		at 350°C		at 510°C		at 970°C	
d(Å)	*I*(Rel)	*d*(Å)	I/I_o(Rel)	*d*(Å)	I/I_o(Rel)	*d*(Å)	I/I_o(Rel)	*d*(Å)	I/I_o(Rel)
0.962	62.40	–	–	1.482	41	2.437	59	1.915	75
0.924	65.27	–	–	1.430	46	2.410	39	1.714	40
0.923	67.04	–	–	1.207	42	2.190	47	1.668	41
0.895	64.71	–	–	1.197	48	1.676	44	1.643	40
0.867	70.54	–	–	1.191	44	1.646	42	1.567	53
0.852	68.88	–	–	–	–	1.598	42	1.482	41
0.831	66.60	–	–	–	–	1.550	41	1.431	43
0.811	67.70	–	–	–	–	1.246	36	1.363	42
0.802	68.22	–	–	–	–	1.218	43	–	–
0.801	66.89	–	–	–	–	1.202	40	–	–
0.786	69.29	–	–	–	–	1.167	36	–	–
–	–	–	–	–	–	1.142	39	–	–
–	–	–	–	–	–	1.114	41	–	–
–	–	–	–	–	–	1.091	32	–	–

with 59.5% mass loss indicates the further changes of oxycarbonate to dioxycarbonate with the formation of mixture residue, CrO and $1/2La_2O_2CO_3$ (mass loss, calcd, 60.17%). A small amount of oxycarbonate also decomposed directly to La_2O_3 at this temperature. The type of DTG changes in the ranges 378–403°C, 403–500°C and 500–540°C correspond to the comprising steps in the whole range of 374 to 550°C in TG. Further, the TG curve is stable in a long temperature range of 550–778°C. The 3% mass gain from 778 to 853°C is due to residual unoxidised C formed, a part of which, in turn, led to metal carbides; or oxidation of a trace of CrO to Cr_2O_3 and CrO_2. A small endotherm at 770°C is responsible for the oxidation and carbides formation. Eventually, 65% mass loss at 1000°C in TG indicates the leading of $1/2Cr_2O_3\cdot 1/2La_2O_3$ ($LaCrO_3$, calcd, 62.38%) or $CrO\cdot 1/2La_2O_3$ ($LaCrO_{2.5}$, calcd, 63.64%) or $LaCrO_2$ (calcd, 64.90%). XRD data of the light greenish pyrolysed species at 970°C in furnace are tabulated in Table 2. It is noticeable that along with the main constituent of chromium, CrO_2, other oxides and carbides i.e., Cr_2O_3 (trace), Cr_3O_4 and Cr_3C_2 (trace) are detected from the *d*-spacing. The recorded *d*-values also confirmed the presence of La_2O_3, La_2C_3, LaCO and C. The remaining mismatched *d*-values are attributed to $LaCrO_x$ ($2<x<3$). The IR bands of the residue also gives evidence of the existence of some of the above species isolated at 970°C.

The DSC profile (Fig. 2) recorded in nitrogen exhibited a large endothermic peak between 132–212°C. This is due to the removal of water molecules accompanied by partial breaking of the anhydrous moiety. A small shoulder endotherm in the range 90–127°C is due to the removal of water molecules in first phase. Furthermore, another small endothermic peak in the range 227–241.7°C, which is overlapped with an exotherm in the range 241.7–295°C, indicates further rearrangement and decom-

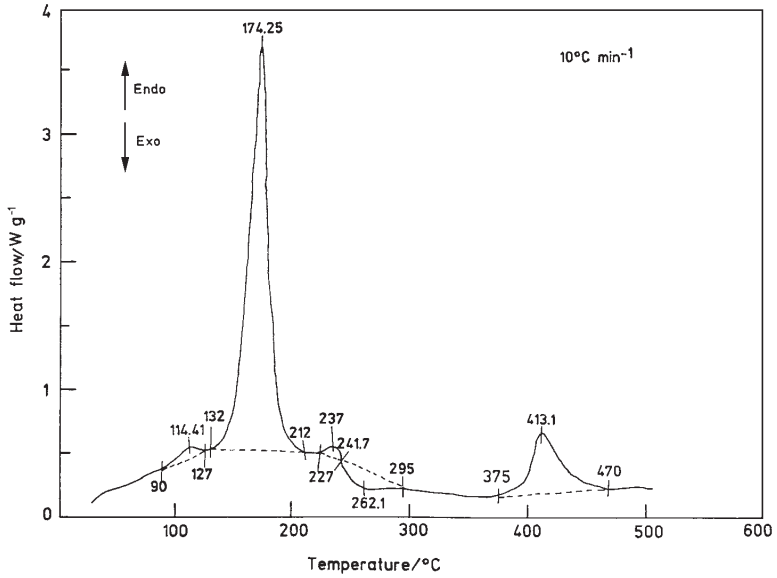

Fig. 2 DSC curves of $Cr[La(C_2O_4)_3]\cdot 10H_2O$ in nitrogen

position of the species formed corresponding to the large endothermic peak. At the end of the scanning an endotherm between 375 to 470°C is due to the main decomposition like the exothermic peak observed in DTA in air. The values of the change of enthalpy (ΔH) and entropy (ΔS) of the steps are included in Table 4. These seem to be dependent on the area of the peaks of the respective changes as shown in Fig. 2.

Table 4 DSC data of $Cr[La(C_2O_4)_3]\cdot 10H_2O$ and $Co[La(C_2O_4)_3]\cdot 7H_2O$ in nitrogen at 10°C min^{-1}

Compound	Step	Temperature range/ °C	Peak/ °C	ΔH/ kJ mol^{-1}	ΔS/ J K^{-1} mol^{-1}
$Cr[La(C_2O_4)_3]\cdot 10H_2O$	1	90–127 (sh, endo)	114.41	2.79	7.21
	2	132–212 (endo)	174.25	239.69	535.92
	3	227–241.7 (sh, endo)	237.00	7.39	14.50
	4	241.7–295 (exo)	262.10		
	5	375–470 (endo)	413.10	51.06	74.43
$Co[La(C_2O_4)_3]\cdot 7H_2O$	1	122–194 (endo)	172.97	92.69	207.85
	2	198–327 (endo)	231.33	138.12	273.87
	3	340–450 (endo)	404.00	90.32	133.41
	4	455–543 (endo)	504.90	19.16	24.63
	5	543–587 (endo)	553.74	4.02	4.86

The foregoing study suggests the following tentative mechanism of thermal decomposition in air,

$$Cr[La(C_2O_4)_3]\cdot 10H_2O \xrightarrow{\text{room temp.–170 °C}} Cr[La(C_2O_4)_3]\ (s)+10H_2O\ (v) \xrightarrow{\sim 374\,^\circ C}$$

$$Cr[La(C_2O_4)_{2.5}]\ (s)+CO\ (g) \xrightarrow{\sim 430\,^\circ C \text{ pyrolysed at } \sim 420\,^\circ C} CrO\ (s)+Cr_2O_3\ (s)\ (\text{trace})+$$

$$+CrO_2\ (s)\ (\text{trace})+La_2O_3\ (s)+1/2La_2(CO_3)_3\ (s)+C\ (s)+1CO\ (g)+mCO_2\ (g) \xrightarrow{\sim 550\,^\circ C}$$

$$CrO\ (s)+1/2La_2O_2CO_3\ (s)+La_2O_3\ (s)+\text{other oxides of chromium}+C\ (s)+pCO\ (g)+$$

$$+qCO_2\ (g) \xrightarrow{1000\,^\circ C \text{ pyrolysed at } \sim 970\,^\circ C} CrO_2\ (s)+Cr_2O_3\ (s)\ (\text{trace})+Cr_3O_4\ (s)+$$

$$+Cr_3C_2\ (s)\ (\text{trace})+La_2O_3\ (s)+La_2C_3\ (s)+LaCO\ (s)+C\ (s)+$$

$$+LaCrO_x\ (s)\ (2<x<3)+xCO\ (g)+yCO_2\ (g)$$

The thermal profile (TG, DTG and DTA) of $Co[La(C_2O_4)_3]\cdot 7H_2O$ are given in Fig. 3. An inclined slope in TG from 35 to 150°C indicates the removal of four molecules of water (mass loss, found, 12; calcd, 12.26%). A break at 100°C indicates the elimination of first water molecule. Another distinct slope from 150 to 225°C (mass loss, found, 21.5%; calcd, 21.5%) is for the detachment of remaining three coordinated water molecules. Two overlapping DTG changes separated as 88–173°C and 173–240°C correspond to the two-step dehydration process. In DTA curve two clear endothermic peaks in the range 90–174°C (ΔT_{min}=138°C) and 174–240°C

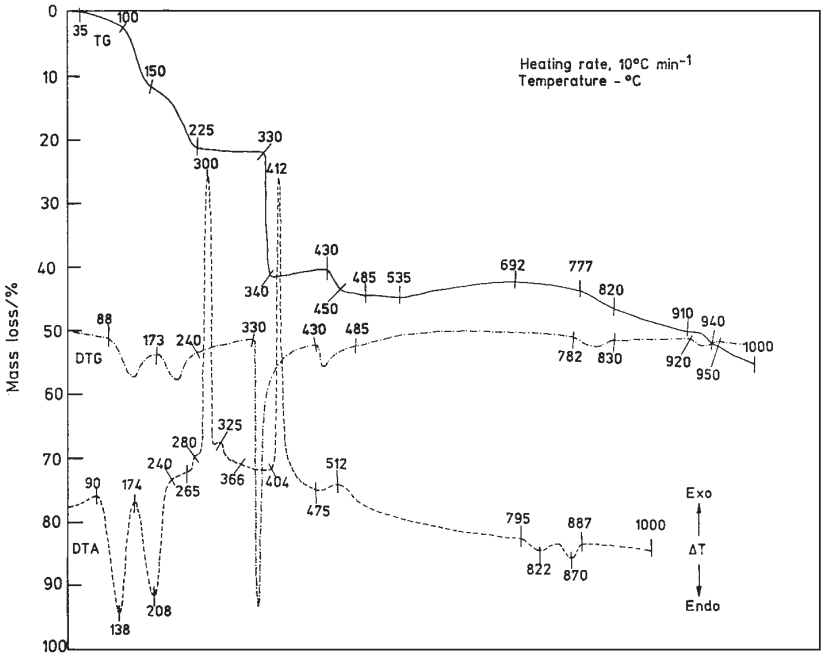

Fig. 3 TG, DTG and DTA curves of $Co[La(C_2O_4)_3]\cdot 7H_2O$ in air

(ΔT_{min}=208°C) corresponded well with the processes. The deaquated form is stable upto 330°C in TG. The pyrolysed product of the precursor at ~257°C in furnace showed the XRD peaks and IR bands. XRD data (Table 3) show some *d*-spacings are in agreement with the precursor. Although the peaks are lower as compared to the precursor due to the structural change on deaquation, of course, the chelation of $C_2O_4^{2-}$ group retains as such. The IR bands support the retention of chelating oxalato groups. The species decomposes to a compound with 42% mass loss corresponding to a steep slope from 330 to 340°C. The observed mass loss apparently supports the compound is a mixture of separated cobalt oxide and lanthanum oxalate as CoO and $1/2La_2(C_2O_4)_3$ (mass loss, calcd, 41.18%), or $1/2Co_3O_4$ and $1/2La_2(CO_3)_3$ (calcd, 40.59%). XRD data (Table 3) of black calcined product at ~350°C do not depict any lines for CoO, IR did not show any band for this either, instead, the vibration at 654, 562, 462 and 350 cm^{-1} gives credence [39] for the existence of Co_3O_4. Besides, XRD data confirmed its presence. Moreover, absence of bands due to characteristic vibrations for $C_2O_4^{2-}$ group indicates its rupture, which supports the absence of lanthanum oxalate. However, the residue when reacted with dil HCl gave effervescence, which is an indication of carbonate, and its presence is substantiated [27, 38, 41] by the presence of some more IR bands at 1350–1550, 1030 and 845 cm^{-1} for CO_3^{2-}. A few additional peaks in XRD may be due to $La_2(CO_3)_3$. In DTA curve a sharp exothermic peak in the range 265–366°C (ΔT_{max}=300°C) with two small shoulders at 280 and 325°C at the respective left and right edge is for the above mentioned decomposition to co-

balt(II, III) oxide and carbonate of lanthanum. A sharp DTG change (330–430°C) is accounted for this decomposition. The first shoulder in DTA is due to the disproportionation [17, 18, 27] of CO (*g*) to CO_2 (*g*) and C during rupture of $C_2O_4^{2-}$. A part of C inturn oxidised to CO_2 (*g*) in accordance with 325°C. 1% mass gain in the range 340–430°C in TG is due to the remaining unoxidised carbon in the residue. XRD data (Table 3) of the products at ~350°C give evidence for its presence. Unlike our earlier study on $La[La(C_2O_4)_3]\cdot 9H_2O$ [17], $Na_3[La(C_2O_4)_3]\cdot 8H_2O$ [26] and $K_3[La(C_2O_4)_3]\cdot 9H_2O$ [27], which decomposed to $La_2O(CO_3)_2$ at 494, 538 and 480°C respectively through some intermediates like $La[La(C_2O_4)_x]$ ($2.5<x<3$), in the present case the anhydrous form first led to Co_3O_4 at 330°C (which formed at 300°C from cobalt oxalate in our earlier study [10]), which immediately acts as a catalyst for early decomposition of $C_2O_4^{2-}$ leading to $La_2(CO_3)_3$ at 340°C in TG. Furthermore, in TG an inclined slope from 430 to 485°C (mass loss, 46%) through a break at 450°C (44% mass loss) is displayed. The observed mass loss as against calculated value of 48.08% for the mixture residue $1/2Co_3O_4$ and $1/2La_2O_2CO_3$, and 51.81% for $1/2Co_3O_4$ and $1/2La_2O_3$ ascertains the presence of some more species. 44% mass loss at 450°C corresponded well with the mixture $1/2Co_3O_4$ and lanthanum oxycarbonate, $1/2La_2O(CO_3)_2$ (calcd, mass loss, 44.33%). The oxycarbonate owing to its transient nature in decomposition mode may immediately change to dioxycarbonate and oxide as reported earlier [17, 27]. The black pyrolysed product at 510°C (as TG curve is stable upto 535°C) is subjected to XRD and IR study. XRD data (Table 3) confirmed the presence of Co_3O_4 and La_2O_3. A few *d*-values coincides with Co_2O_3 indicating its presence in trace. Moreover, some *d*-spacing is in excellent agreement with carbides of cobalt, Co_2C and Co_3C, and lanthanum carbide, La_2C_3 and oxycarbide, LaCO as well. The carbides of various metals are also found in earlier studies [17, 18, 26, 27]. These are formed through the reaction of unoxidised C with some part of molten oxides of metal at high temperatures. The observed IR bands at 654, 645, 560, 412 and 350 cm^{-1} further support [39] the presence of Co_3O_4, Co_2O_3 and La_2O_3. The bands at 1480 and 1028 cm^{-1} are for CO_3^{2-} group of oxycarbonate. The DTG change in the range 430–485°C, and an exotherm in DTA between 404 to 475°C (ΔT_{max}=412°C) correspond to the above decomposition and plausible rearrangement through various interactions among the products. The exothermal nature of DTA curve at 512°C without change in TG and DTG in the range 485–535°C may be due to some phase changes or change of crystallinity of the products [13, 17]. Subsequent gain of mass of 3% from 535 to 692°C in TG curve is observed. This is due to the fact that with the increase of temperature a continuous solid-solid interaction of the products leads to new products. The free unoxidised and unreacted carbon led through disproportionation of evolved CO (*g*) may also increase the mass of residue. Eventually, the continuous mass loss from 692 to 1000°C indicates the formation of product such as $LaCoO_3$ (mass loss, found, 56.5; calcd, 58.19%). The remarkable difference in mass loss indicates the presence of other species. XRD data (Table 3) of the pyrolysed product around 970°C in furnace confirmed the presence of $LaCoO_3$, Co_3O_4 and La_2O_3. Free C in trace is also detected. IR bands further substantiate the presence of

Co_3O_4 and La_2O_3. Prior to the formation of the end product a clear step in TG in the range 777–820°C, and a change between 782 and 830°C in DTG are displayed. Another distinct step in TG (910–940°C with 53% mass loss) corresponds to a DTG change in the range 920–950°C is noticed, which may be ascribed due to interaction of Co_3O_4/Co_2O_3 and La_2O_3 leading to $LaCoO_3$ as one of the end products. The two overlapping endothermic peaks in DTA in the range 795–887°C (ΔT_{min} of 822 and 870°C) are responsible for the interaction phenomena corresponded to two changes in TG mentioned.

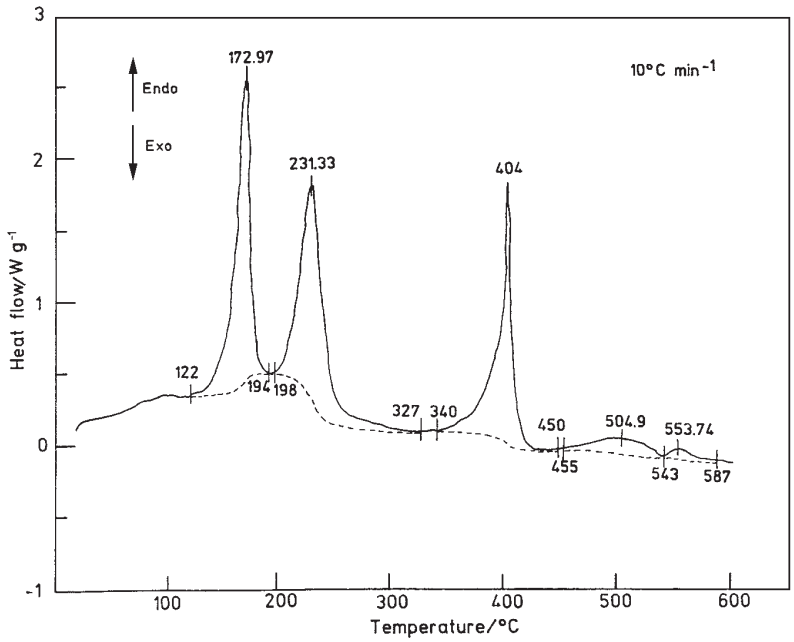

Fig. 4 DSC curves of $Co[La(C_2O_4)_3]\cdot 7H_2O$ in nitrogen

The DSC profile of the compound in nitrogen is shown in Fig. 4. The curve upto 600°C shows three large endothermic peaks followed by two small endotherms. The first two endotherms in the ranges 122–194 and 198–327°C correspond to the two-step dehydration as in air. The third endothermic peak between 340 and 450°C is due to the decomposition of the anhydrous species. The oxidation of CO (*g*) evolved during decomposition is not perceptible in inert atmosphere, which keeps the step as endothermic. The product formed corresponds to the third endotherm is changed or rearranged which is supported by subsequent two small endotherms between 455 to 587°C with a peak temperature of 504.9 and 553.74°C. ΔH and ΔS values of the endotherms (Table 4) depend on the area of the respective changes as observed in $Cr[La(C_2O_4)_3]\cdot 10H_2O$. The mass loss at the end of the scan is found to be 43.95%, which indicates the formation of $1/2Co_3O_4$ and $1/2La_2O(CO_3)_2$ (calcd, 44.33%).

The tentative decomposition scheme in air is shown below

$$Co[La(C_2O_4)_3]\cdot 7H_2O \xrightarrow{35-150\,^\circ C} Co[La(C_2O_4)_3]\cdot 3H_2O\ (s)+4H_2O(v) \xrightarrow{150-225^\circ C}$$

$$Co[La(C_2O_4)_3]\ (s)+3H_2O\ (v) \xrightarrow{330-340\,^\circ C \text{ pyrolysed product at } \sim 348\,^\circ C} 1/2Co_3O_4\ (s)+$$

$$+1/2La_2(CO_3)_3\ (s)+C\ (s)+lCO\ (g)+mCO_2\ (g) \xrightarrow{430-485^\circ C \text{ pyrolysed product at } \sim 510\,^\circ C}$$

$$1/2Co_3O_4\ (s)+$$

$$+1/2La_2O_3\ (s)+Co_2O_3\ (s)\ (\text{trace})+1/2La_2O(CO_3)_2\ (s)/1/2LaO_2CO_3\ (s)+$$

$$+Co_2C\ (s)/Co_3C\ (s)+La_2C_3\ (s)+LaCO\ (s)\ (\text{trace})+C\ (\text{trace})+pCO\ (g)+qCO_2\ (g)$$

$$\xrightarrow{1000\,^\circ C \text{ pyrolysed product at } \sim 970\,^\circ C} LaCoO_3\ (s)+Co_3O_4\ (s)\ (\text{trace})+La_2O_3\ (s)\ (\text{trace})+$$

$$+La_2C_3\ (\text{trace})+Co_3C\ (\text{trace})+LaCO+C\ (\text{trace})+xCO\ (g)+yCO_2\ (g)$$

* * *

The author thankful to Dr. S. D. Baruah, Regional Research Laboratory, Jorhat for the DSC profile.

References

1 K. V. Krishnamurty and G. M. Harris, Chem. Rev., 61 (1961) 213.
2 D. Dollimore, D. L. Griffiths and D. Nicholson, J. Chem. Soc., (1963) 2617.
3 W. W. Wendlandt and E. L. Simmons, J. Inorg. Nucl. Chem., 27 (1965) 2317.
4 D. Broadbent, D. Dollimore and J. Dollimore, J. Chem. Soc., A, (1967) 451.
5 G. M. Bancroft, K. G. Dharmawardena and A. G. Maddock, Inorg. Chem., 9 (1970) 223.
6 K. Nagase, K. Sato and N. Tanaka, Bull. Chem. Soc. Jpn., 48 (1975) 868.
7 A. E. Underhill and D. M. Watkins, Chem. Soc. Rev., 9 (1980) 429.
8 T. K. Sanyal and N. N. Dass, J. Inorg. Nucl. Chem., 42 (1980) 811.
9 N. Deb, P. K. Gogoi and N. N. Dass, Bull. Chem. Soc. Jpn., 61 (1988) 4485.
10 N. Deb, P. K. Gogoi and N. N. Dass, J. Thermal Anal., 35 (1989) 27.
11 N. Deb, P. K. Gogoi and N. N. Dass, Thermochim. Acta, 140 (1989) 145.
12 N. Deb, P. K. Gogoi and N. N. Dass, Thermochim. Acta, 145 (1989) 77.
13 N. Deb, P. K. Gogoi and N. N. Dass, J. Thermal Anal., 36 (1990) 465.
14 N. Deb, P. K. Gogoi and N. N. Dass, Thermochim. Acta, 198 (1992) 395.
15 N. Deb, S. D. Baruah and N. N. Dass, J. Thermal Anal., 45 (1995) 457.
16 N. Deb, S. D. Baruah and N. N. Dass, Thermochim. Acta, 285 (1996) 301.
17 N. Deb, S. D. Baruah, N. Sen Sarma and N. N. Dass, Thermochim. Acta, 320 (1998) 53.
18 N. Deb, S. D. Baruah, N. Sen Sarma and N. N. Dass, Thermochim. Acta, 329 (1999) 129.
19 S. K. Awasthi, K. L. Chawla and D. M. Chakraburty, J. Inorg. Nucl. Chem., 36 (1974) 2521.
20 H. S. Gopalakhrishna-Murthy, M. Subba Rao and T. R. Narayanan Kutty, J. Inorg. Nucl. Chem., 37 (1975) 1875.
21 H. S. Gopalakhrishna-Murthy, M. Subba Rao and T. R. Narayanan Kutty, J. Inorg. Nucl. Chem., 38 (1976) 417.
22 B. D. Dalvi and A. M. Chavan, J. Thermal Anal., 14 (1978) 331.
23 M. Verdaguer, M. Julve, A. Michalowicz and O. Khan, Inorg. Chem., 22 (1983) 2624.
24 A. S. Brar, S. Brar and S. S. Sandhu, J. Thermal Anal., 31 (1986) 1083.
25 M. G. Usha, M. Subba Rao and T. R. Narayanan Kutty, J. Thermal Anal., 31 (1986) 7.

26 N. Deb, S. D. Baruah and N. N. Dass, Thermochim. Acta, 326 (1999) 43.
27 N. Deb, Thermochim. Acta, 338 (1999) 27.
28 K. Nagase, Chem. Lett. Jpn., 7 (1972) 587.
29 K. Nagase, Bull. Chem. Soc. Jpn., 46 (1973) 144.
30 N. W. Alcock, J. Chem. Soc. Dalton Trans., (1973) 1614.
31 N. D. Dahale, K. L. Chawla, N. C. Jayadevan and V. Venugopal, Thermochim. Acta, 293 (1997) 163.
32 K. Nag and Ajoy Roy, Thermochim. Acta, 17 (1976) 247.
33 Om Prakash, P. Ganguly, G. Rama Rao, C. N. R. Rao, V. G. Bhide and D. S. Rajoria, Mater. Res. Bull., 7 (1974) 1173.
34 Yung-Frang Yu. Yao, J. Catal., 36 (1975) 266.
35 D. J. Anderton and F. R. Sale, Powder Metall., 22 (1979) 14.
36 N. Deb, S. D. Baruah and N. N. Dass, J. Therm. Anal. Cal., 59 (2000) 791.
37 F. A. Cotton and G. Wilkinson, Advanced Inorganic Chemistry, 5th ed., Wiley, New York 1988, p. 734.
38 M. G. Usha, M. Subba Rao and T. R. Narayanan Kutty, Thermochim. Acta, 43 (1981) 35.
39 F. F. Bentley, L. D. Smithson and A. L. Rozek, Infrared Spectra and Characteristic Frequencies, 300–700 cm^{-1} , Wiley, New York 1968.
40 K. Nakamoto, Infrared Spectra of Inorganic and Coordination Compounds, 2nd ed., Wiley, New York 1969, p. 245.
41 R. P. Turcotte, J. D. Sawyer and L. Eyring, Inorg. Chem., 8 (1965) 238.
42 Joint Committee on Powder Diffraction Standards, Inorganic Index to the Powder Diffraction File, 1971, 1601, Parklane, Pennsylvania.